Active site restructuring regulates ligand recognition in class A penicillin-binding proteins

Pauline Macheboeuf[†], Anne Marie Di Guilmi[‡], Viviana Job[†], Thierry Vernet[‡], Otto Dideberg[†], and Andréa Dessen[†§]

Laboratoires [†]de Cristallographie Macromoléculaire and [‡]d'Ingénierie des Macromolécules, Institut de Biologie Structurale Jean-Pierre Ebel, Centre National de la Recherche Scientifique/Commissariat à l'Energie Atomique/Université Joseph Fourier, 41 Rue Jules Horowitz, 38027 Grenoble, France

Edited by Christopher T. Walsh, Harvard Medical School, Boston, MA, and approved December 1, 2004 (received for review September 29, 2004)

Bacterial cell division is a complex, multimolecular process that requires biosynthesis of new peptidoglycan by penicillin-binding proteins (PBPs) during cell wall elongation and septum formation steps. *Streptococcus pneumoniae* has three bifunctional (class A) PBPs that catalyze both polymerization of glycan chains (glycosyltransfer) and cross-linking of pentapeptidic bridges (transpeptidation) during the peptidoglycan biosynthetic process. In addition to playing important roles in cell division, PBPs are also the targets for β-lactam antibiotics and thus play key roles in drug-resistance mechanisms. The crystal structure of a soluble form of pneumococcal PBP1b (PBP1b*) has been solved to 1.9 Å, thus providing previously undescribed structural information regarding a class A PBP from any organism. PBP1b* is a three-domain molecule harboring a short peptide from the glycosyltransferase domain bound to an interdomain linker region, the transpeptidase domain, and a C-terminal region. The structure of PBP1b* complexed with β-lactam antibiotics reveals that ligand recognition requires a conformational modification involving conserved elements within the cleft. The open and closed structures of PBP1b* suggest how class A PBPs may become activated as novel peptidoglycan synthesis becomes necessary during the cell division process. In addition, this structure provides an initial framework for the understanding of the role of class A PBPs in the development of antibiotic resistance.

antibiotic | cell wall | transpeptidase | glycosyltransferase

Streptococcus pneumoniae is a major human pathogen, being the causative agent of pneumonia and meningitis, which victimize >1 million individuals yearly, especially in developing countries. Treatment of such infections has, for >60 years, depended on β-lactam antibiotics, which perturb the cell wall biosynthetic machinery by targeting penicillin-binding proteins (PBPs). PBPs catalyze the last steps in the synthesis of the peptidoglycan, a 3D cross-linked mesh composed of repeating disaccharide units linked to peptidic bridges (1); stability of the peptidoglycan not only is necessary for bacterial shape and morphology, but its synthesis is an absolute requirement for normal cell division and growth processes. Thus, targeting of the peptidoglycan biosynthetic machinery by β-lactams often leads to cell lysis and death.

The dissection of the functions of PBPs within growth and division processes has proven to be challenging in microorganisms such as *Escherichia coli*, which has 12 PBPs, and *Bacillus subtilis*, whose 7 PBPs also participate in sporulation. *S. pneumoniae* has six PBPs, three of which catalyze both glycosyltransfer and transpeptidation of the peptidoglycan (PBPs 1a, 1b, and 2a; class A), two of which catalyze uniquely the transpeptidation reaction (PBPs 2x and 2b; class B), and PBP3, which acts as a *D*,*D*-carboxypeptidase (2).

In the bacterial cell cycle, peptidoglycan synthesis occurs during two major stages: wall elongation and cell division, or septation. Septation starts once FtsZ, the bacterial homolog of tubulin, polymerizes in the form of a contractile ring at the future division site, and ≈12 proteins are recruited subsequently in a defined order at the site of the constricting ring (3). Each of the two processes has been shown to specifically require one class A and one class B PBP: The elongation process involves PBP2a and PBP2b in *S. pneumoniae*, whereas division involves PBP1a and PBP2x. In *S. pneumoniae*, PBP1b, the third class A molecule, was shown to participate both in elongation and septation but never in the same cell (4); in addition, inactivation of PBP1b together with either of the two other class A enzymes yielded viable strains with defects in septum positioning (5) or that displayed slower growth than the wild-type (WT) strain (6). These observations suggest that there is a precise, but not yet fully understood, role for class A PBPs in the cell-division process.

Class A PBPs are membrane-associated enzymes that harbor both glycosyltransferase (GT) and transpeptidase (TP) activities on the same polypeptide in the form of distinct domains identifiable by classic motifs. Thus, these enzymes are optimally constructed to catalyze the concerted polymerization of *N*-acetylmuramic acid-β-1,4-GlcNAc moieties and cross-linking of stem peptides by employing the periplasmically located lipid II as substrate (2). The GT domain is of particular interest because it may harbor a yet-uncharacterized fold and thus could be a novel potential antibacterial development target (7). In addition, certain class A PBPs are involved in the development of antibiotic resistance (8–10). Despite their importance in cell division and antibiotic-resistance processes, as well as their potential application in the drug-development industry, structural information regarding class A PBPs has to date remained elusive. In this work, we report the crystal structure of a class A PBP, that of a soluble form of PBP1b (PBP1b*) from *S. pneumoniae*. PBP1b* harbors a short peptide from the N terminus of the GT domain, the entire interdomain junction region, and the TP domain, followed by a small C-terminal region. Interestingly, PBP1b* displays a closed, inaccessible active cleft in the absence of ligand, whereas a large conformational modification, involving loop movement and repositioning of key catalytic elements, is observed in the active site in the presence of antibiotics. These observations suggest that PBPs may exist in inactive conformations during phases of the cell-division cycle in which they do not participate, becoming activated only as needed. In addition, the structure also provides insight into drug-resistance mechanisms generated by mutant class A PBPs.

Materials and Methods

Sample Preparation. PBP1b* was purified as described in ref. 11. This procedure generated a protein product with three proteolytic sites (following Arg-336, -686, and -687). These sites were mutated into glutamines (QuikChange, Stratagene), and mutant protein was purified by employing the same strategy as described for the WT enzyme. This preparation, henceforth called PBP1b*, contained peptides Asp-101–Arg-125 and Gly-306–Pro-791 (verified by N-terminal sequencing and native mass spectrometry) and was used for crystallization trials.

This paper was submitted directly (Track II) to the PNAS office.

Abbreviations: PBP, penicillin binding protein; GT, glycosyltransferase; TP, transpeptidase; S2d, *N*-benzoyl-D-alanylmercaptoacetic acid.

Data deposition: The atomic coordinates and structure factors have been deposited in the Protein Data Bank, www.pdb.org [PDB ID codes 2bg1 (PBP1b*), 2bg3 (PBP1b*-nitrocefin), and 2bg4 (PBP1b*-cefotaxime)].

[§]To whom correspondence should be addressed. E-mail: dessen@ibs.fr.

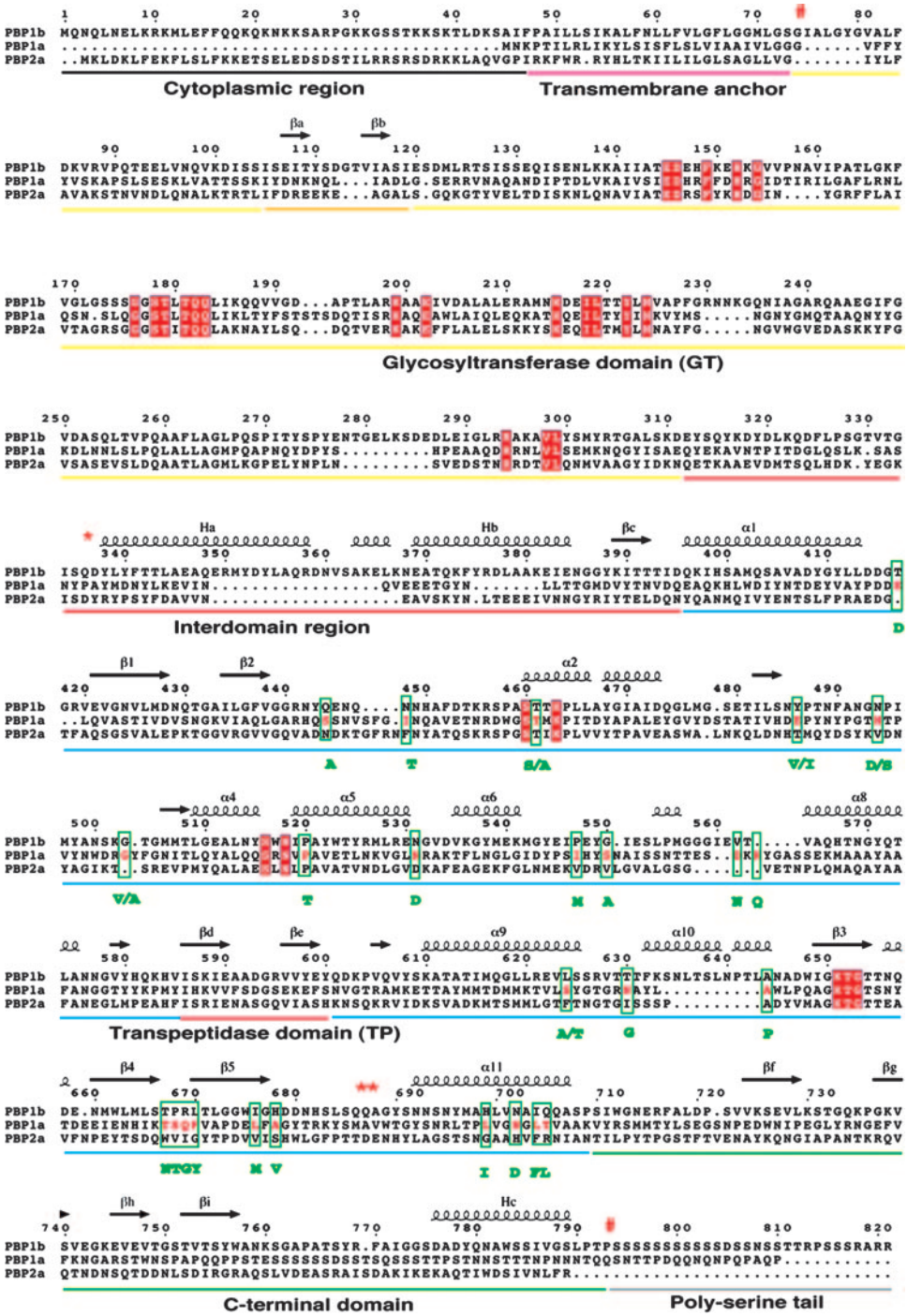

Fig. 1. Sequence alignment of class A PBPs from *S. pneumoniae*, strain R6. The secondary structure elements of PBP1b* are shown over the sequences. Conserved motifs are shown inside red boxes. The three mutations introduced into PBP1b are identified with red ''X'' marks. The beginning and ends of the full-length clone are shown with #. Residues mutated in a PBP1a from streptococcal clinical resistant strain 8303 (described in ref. 9) are surrounded by green boxes; mutations are shown underneath.

Crystallization and Data Collection. Crystals of PBP1b* were obtained by the hanging-drop vapor-diffusion method by mixing 1 μl of the protein sample (6.4 mg/ml in 20 mM Hepes, pH 7.0/100 mM NaCl/1 mM EDTA) with 1 μl of 50 mM Hepes, pH 7.0/0.8 M $(NH_4)_2SO_4$/2.8 M NaCl at 15°C. Before data collection, each crystal was briefly immersed in a cryoprotectant solution containing 20% ethylene glycol and flash-cooled in liquid nitrogen. A native data set was collected to 1.9 Å at the European Synchrotron Radiation Facility BM30 beamline (Grenoble); crystals belonged to space group $C222_1$.

Selenomethionine-derivatized PBP1b* crystals were grown in conditions similar to those used for the native protein. No antibiotic-complexed crystals were obtained by either (*i*) incubating native crystals in the presence of high amounts of antibiotics, or (*ii*) attempting to cocrystallize PBP1b* with different antibiotics. Nitrocefin- and cefotaxime-soaked crystals were obtained only after washing native crystals that had been complexed previously to *N*-benzoyl-D-alanylmercaptoacetic acid (S2d) in ligand-free mother liquor and subsequently incubating them with 3 μl of 633 μM nitrocefin or 320 μM cefotaxime for 3 h. S2d-complexed crystals

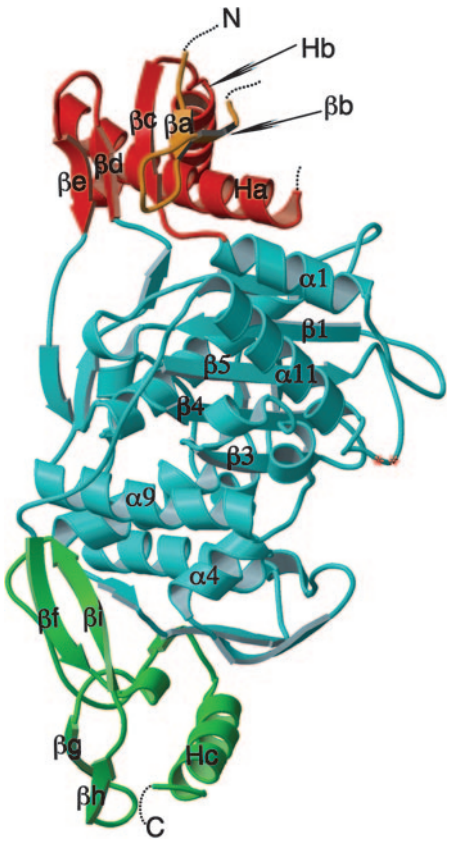

Fig. 2. Tertiary fold of PBP1b*. The TP domain (center, blue) is flanked by the GT/TP interdomain region (red) and a peptide from the GT domain (top, orange) as well as the C-terminal domain (bottom, green). From this point of view, the active site is located between β3 and α4. The residues that are not visible in the electron density map are represented as dotted lines.

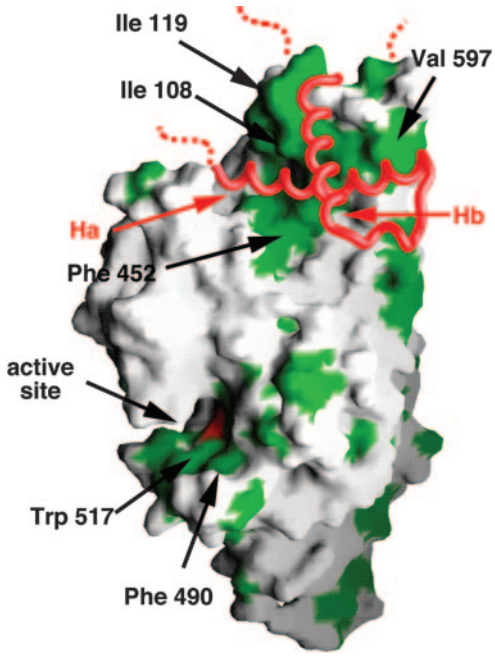

Fig. 3. Surface representation of PBP1b*, with the GT/TP interdomain linker region shown as a red C^{α}. Hydrophobic residues are shown in green.

were obtained by mixing 16 μl of PBP1b* (12.7 mg/ml in 20 mM Hepes, pH 7.0/100 mM NaCl/1 mM EDTA) with 8 μl of 15 mM S2d and allowing a 5-min reaction time. Subsequently, 1 μl of the protein/S2d mixture was mixed with 1 μl of 50 mM Hepes (pH 7.0), 0.8 M $(NH_4)_2SO_4$, and 2.8 M NaCl at 15°C, and crystals were obtained by the hanging-drop vapor-diffusion method using the latter solution as mother liquor. Cryoprotection was performed in 12% ethylene glycol. Data were collected at European Synchrotron Radiation Facility beamlines BM30 (S2d, nitrocefin) and ID14-EH2 (cefotaxime). All data were processed with the programs DENZO and SCALEPACK (12).

Determination of Native and Complex Structures. The structure of PBP1b* was solved by multiple anomalous dispersion by using data collected on the Se edge. We located 16 Se sites in the asymmetric unit and used them for phase determination at 2.4 Å with the program SOLVE (13); phases were subsequently improved, and solvent flattening was performed with the program RESOLVE (14). A model constructed into this electron density map was used in a molecular replacement experiment with the 1.9-Å data set (AMORE; ref. 15). Energy minimization, temperature factor refinement, and simulated annealing steps were performed with the program CNS (16), and manual model improvement was achieved with the program QUANTA (Molecular Simulations, Waltham, MA). Structures of S2d- and antibiotic-complexed crystals were solved by employing the 1.9-Å-data-derived model that lacked the active site gorge, including β3, β4, α4, α5, and the N-terminal region of α2 (15). The S2d complex structure showed poor ligand density and thus is not further discussed. However, these crystals were useful for the preparation of complexes with antibiotics, because direct soaking or cocrystallization attempts of PBP1b* with β-lactams were unsuccessful. The native, nitrocefin, and cefotaxime structures displayed 99.4%, 99.3%, and 98% of the nonglycine residues, respectively, in the most favored and allowed regions of the Ramachandran plot (PROCHECK; ref. 17). Molecule B in the PBP1b*-cefotaxime structure lacks 20 residues at the N termini of Ha and Hb. Statistics for data collection and structure refinement are included in *Supporting Text* and Tables 2 and 3, which are published as supporting information on the PNAS web site.

Results

Overall Structure. PBP1b from *S. pneumoniae* contains a short cytoplasmic region and an N-terminal membrane anchor, followed by a 25-kDa GT joined to a 50-kDa TP domain through a long linker region (Fig. 1). In the absence of diffracting crystals of the full-length, soluble form of PBP1b, attempts were made to produce a stable form through trypsinolysis of the molecule. This procedure generated a soluble fragment with three internal cleavage sites (11), which yielded only microcrystalline precipitate. Mutagenesis of these sites yielded a stable form of PBP1b (PBP1b*) that produced high-quality crystals that were used for structure determination by multiple anomalous dispersion using selenomethionyl-substituted protein. The crystallized PBP1b* is composed of two associated polypeptides: Gly-306–Pro-791, which encompasses the GT/TP junction region (residues 306–396), the TP domain (residues 397–710), and a small C-terminal region (residues 711–791); and Asp-101–Arg-125, a peptide derived from the N terminus of the GT domain that remained bound to the rest of the molecule after tryptic cleavage and purification.

PBP1b* is a three-domain molecule: the N-terminal domain contains the GT peptide and the GT/TP interdomain region (red in Figs. 1 and 2); the central region harbors the TP domain (blue in Figs. 1 and 2); and at the C terminus there is small, β-strand-rich terminal region (green in Figs. 1 and 2) with no structural similarity in searched databases. At the N terminus, the GT peptide (of which only residues 105–119 are traceable) folds into two short β strands (βa and βb; orange in Fig. 2), which are part of a five-stranded β sheet, with other strands being contributed by the TP domain. The

BIOCHEMISTRY

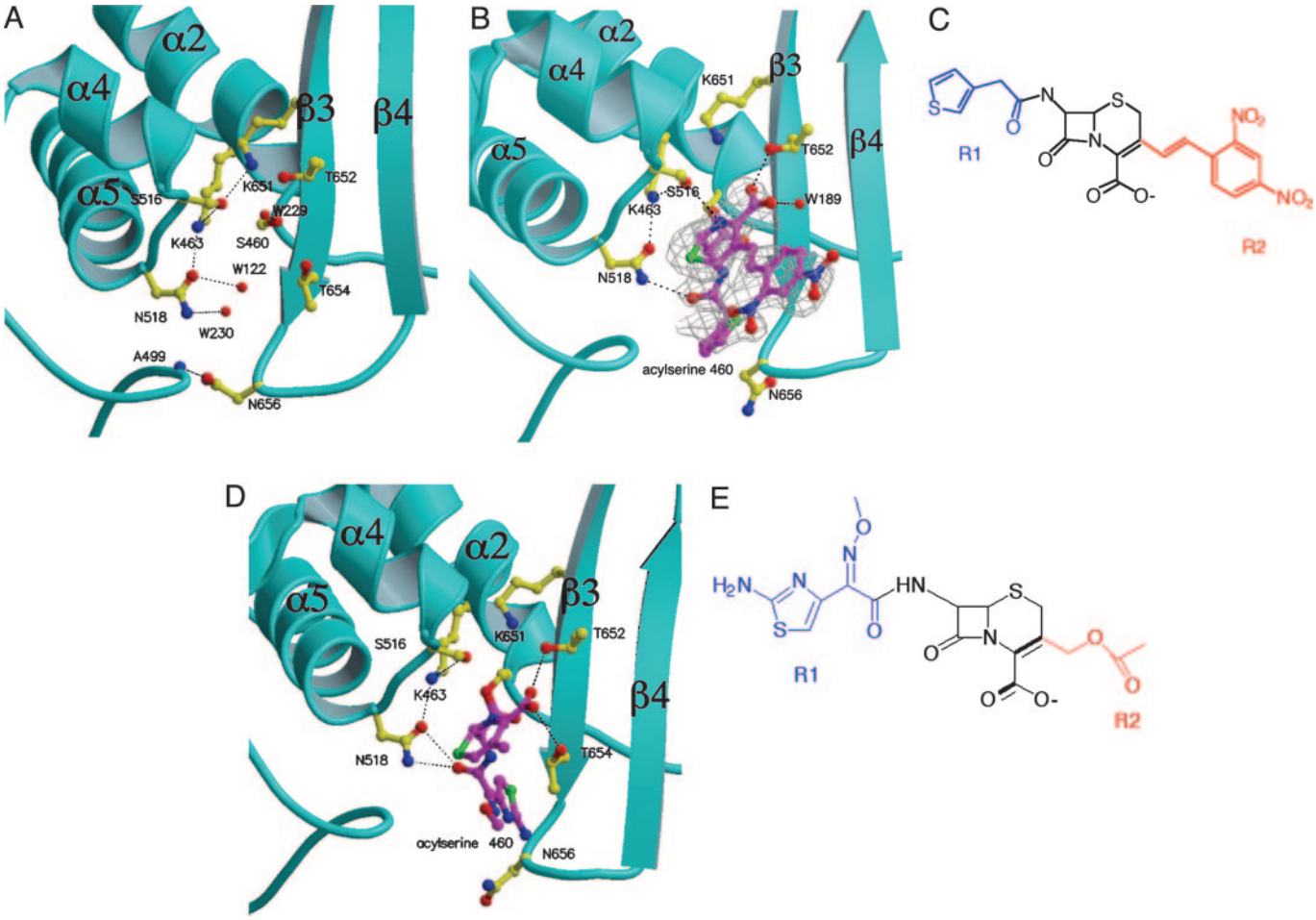

Fig. 4. The PBP1b* active site. (*A*) In the native structure, β3 moves away from β4, and their interconnecting loop closes the active site gorge. (*B*) PBP1b*-acyl-nitrocefin complex. An $F_o - F_c$ omit map contoured at 2.3 σ is shown. (*C*) The chemical structure of nitrocefin. (*D*) PBP1b*-acyl-cefotaxime complex. (*E*) The chemical structure of cefotaxime before acylation.

GT/TP interdomain region is composed of two perpendicular helices (Ha/Hb) separated by a turn. Interestingly, Ha/Hb is stabilized by a hydrophobic funnel (green in Fig. 3) generated by residues Leu-426, Phe-452, Ile-586, Val-597, and Tyr-598, among others, which are positioned laterally on the TP domain, as well as Ile-108, Val-115, Ile-116, and Ile-119, which are contributed by the GT peptide on the five-stranded β-sheet. In Fig. 3, dotted lines represent sequences within the GT domain that are missing from the structure. Notably, Ha, which immediately follows the C terminus of the missing GT domain, is packed snugly within the hydrophobic funnel, whereas Hb is more solvent-exposed. It is of note that binding of the interdomain region on the funnel does not completely cover the hydrophobic patch, and a variety of hydrophobic residues, contributed by the five-stranded β-sheet and the N terminus of Ha, remain solvent-exposed. This organization may provide a hydrophobic recognition patch for the full-length GT domain (see below).

The central region of the molecule harbors the TP domain, which carries the classical signature of the penicilloyl serine transferase superfamily. This domain can be described by a central, antiparallel β-sheet composed of five strands (β3/β4/β5/β1/β2) sandwiched between three α helices [α1 and α11 on one side and α8 on the opposite side of the sheet (blue in Fig. 2)]; the numbering scheme follows that used for class A β-lactamases (18). This fold is found in other β-lactam and peptidoglycan-recognizing enzymes, such as class A β-lactamases (18), the *Streptomyces* K15 transpeptidase (19), and class B PBPs (20–22), albeit with low sequence identities. Superposition of the C^{α} trace of the TP domain of PBP1b* with that of PBP2x (287 C^{α} pairs), K15 (182 C^{α} pairs), and TEM-1 β-lactamase (233 C^{α} pairs) yielded rms deviation values of 2.9, 3.0, and 3.4 Å, respectively, revealing significant structural differences.

Active Site Flexibility Regulates Antibiotic Binding. The TP active site of PBP1b* harbors three conserved structural motifs: SXXK (Ser-460–Thr-461–Thr-462–Lys-463), which includes the nucleophilic Ser-460 residue and is located at the N-terminal end of helix α2; SXN (Ser-516–Trp-517–Asn-518), which forms the turn between helices α4 and α5 on the left side of the cavity; and KTG (Lys-651–Thr-652–Gly-653), which lines strand β3 (Fig. 4*A*). Surprisingly, the active site cavity of PBP1b* contains a major difference from any other of the above-mentioned enzymes in that it is unequivocally unavailable for ligand binding. The interactions between the C terminus of β3 (Thr-654) and the N-terminal region of β4 are disrupted by movement of the intervening loop into the active site region. The stability of this form is such that the C terminus of β3 is "pulled" away from β4, disrupting the local antiparallel nature of the two strands. As a consequence, the side chain of Asn-656 blocks entry into the catalytic cleft and forms a hydrogen bond with the backbone nitrogen of Ala-499, located on the facing loop. Moreover, the O^{γ} atom of the active site serine (Ser-460) contacts backbone atoms of β3 and does not interact with any of the canonical catalytic residues.

To biochemically characterize the unusual active site of PBP1b*, acylation of the enzyme by β-lactam antibiotics was measured by

Table 1. Acylation constants (k_2/K) for binding of different antibiotics to PBP1b* and PBP1b

Antibiotic	PBP1b* (101–125; 306–791)	FL PBP1b* (74–791)	FL PBP1b WT (74–791)
Cephalothin	90.8 ± 3.2	85.3 ± 3.9	253.8 ± 20.0
Cefotaxime	7.8 ± 0.4	7.0 ± 0.2	44.2 ± 1.9
Penicillin G	6.5 ± 0.3	5.0 ± 0.2	19.1 ± 1.8
Nitrocefin	99.7 ± 10.0	ND	ND

Values are $\times 10^3$ $m^{-1}\cdot s^{-1}$ (means ± SD). ND, not determined.

stopped-flow techniques. k_2/K acylation constants are comparable to those obtained for other PBPs (23, 24) and are shown in Table 1. Stabilities of the antibiotic–enzyme complexes were assayed by electrospray ionization-MS, which yielded approximate k_3 values of 1.5 h^{-1} and >24 h^{-1} for nitrocefin and cefotaxime, respectively. These studies clearly indicated that PBP1b* is catalytically active, and thus the catalytic TP domain gorge should be amenable to modification by the presence of a ligand.

To test this hypothesis, crystals of PBP1b* were prepared in the presence of antibiotics nitrocefin and cefotaxime. Cocrystals were obtained in two different space groups ($C222_1$ and $P2_12_12_1$) by employing the same crystallization solution. The nitrocefin-acyl-PBP1b* and cefotaxime-acyl-PBP1b* structures reveal that the products are covalently associated to the O^γ atom of Ser-460, which then points into the active site (Fig. 4 *B–E*). In both structures, the backbone nitrogen atoms of Ser-460 and Thr-654 form the conserved oxyanion hole. The carboxylate group of nitrocefin (Fig. 4*B*) is stabilized by the O^γ atom of Thr-652 as well as by a stably positioned water molecule. The O^γ atom of Ser-516 forms a hydrogen bond with the leaving group nitrogen. In addition, the R1 moiety of nitrocefin is wedged between Asn-656 and -518 and makes van der Waals contacts with the loop composed of residues 496–500 (thus stabilizing the left side of the cavity).

Although cefotaxime only has an exomethylene (CH_2) group as R2 moiety after acylation, its carboxylate group on the β-lactam ring is hydrogen-bonded to the O^γ atoms of both Thr-652 and -654; in addition, the carbonyl group is stabilized by Asn-518 (Fig. 4*D*). Thus, both antibiotics are capable of accessing the active site serine, suggesting that the closed PBP1b* active site is only a transient form of the enzyme. Importantly, in both ligand-bound structures, the conformation of β3 is reestablished, in that it is stably positioned in antiparallel fashion to β4 in its entirety, and the loop that connects the two strands moves away from the gorge, generating an "open," or activated, active site cleft (Fig. 4 *B* and *D*). Active site opening thus reveals an elongated recognition cleft that could accommodate one or two arms of a peptidoglycan stem peptide (compare *A* and *B* in Fig. 5).

Figure Preparation. Figures were prepared with the programs MOLSCRIPT (30), BOBSCRIPT (31), GRASP (32), and ESPRIPT 2.2 (33).

Discussion

Class A PBPs are membrane-associated enzymes ubiquitous to all peptidoglycan-producing bacteria and are responsible for both the polymerization of glycan chains and transpeptidation of stem peptides, the last steps of peptidoglycan biosynthesis. Because novel peptidoglycan production is an essential phase of cell division and growth, class A PBPs play important roles in both processes. *S. pneumoniae* has three class A PBPs, which have proven to be challenging for both biochemical and structural studies. In this paper, we describe the crystal structure of a soluble form of a pneumococcal class A PBP (PBP1b*) that folds as three intimately interacting domains but lacks most of the GT region, except for a N-terminal, 25-residue peptide that remained associated to the body of the molecule after proteolysis and whose central region (residues 105–119) interacts with the GT/TP interdomain region

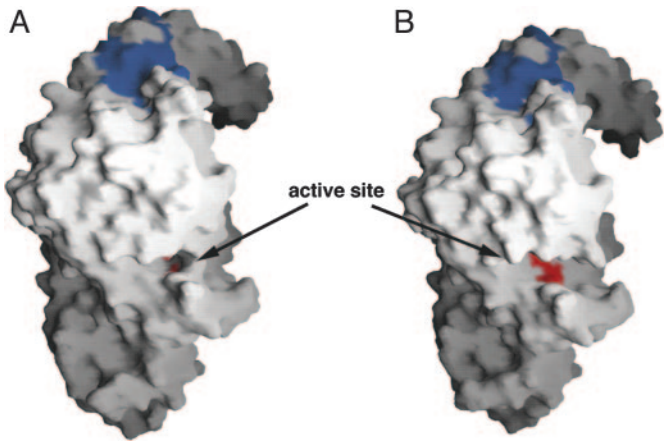

Fig. 5. Surface representation of PBP1b* in closed and open conformations. (*A*) In the closed conformation, the active site is blocked and unavailable for binding. (*B*) Opening of the catalytic gorge reveals an elongated binding cleft with the active site (shown in red) at the bottom. A surface-exposed hydrophobic patch could stabilize the GT domain and position it axially with respect to the TP active site.

through hydrophobic contacts (see Fig. 3). The proximity of the peptide to the GT/TP interdomain region, as well as the presence of a number of solvent-exposed hydrophobic residues in both areas (blue in Fig. 5), allow us to propose that the small, full-length GT domain may interact with the hydrophobic patch formed by these two regions. Thus, in the full-length PBP, the GT domain could be accommodated on the same side of the molecule as the TP active site.

The high similarity in k_2/K values measured for PBP1b* and for the full-length form of the mutated enzyme (FL PBP1b*; Table 1) suggests that the affinity of the molecule for antibiotics is not dependent on the presence of the GT domain, a behavior shared by pneumococcal PBP1a (23). Interestingly, however, the WT, full-length enzyme (FL PBP1b) displays second-order rate constants that range between 2.8- and 6.3-fold higher than for PBP1b* and FL PBP1b* and which harbor Arg → Gln mutations at positions 336, 686, and 687. All three mutant residues are located >20 Å from the active site serine; however, Arg-686 and -687 are located on the loop between β5 and α11 on the TP domain (red asterisks in Fig. 2). In the WT enzyme, their surface exposure could enable their side chains to stabilize the negative charge present on incoming antibiotics, which would not be possible once they are mutated into glutamines. This factor could explain the small observed difference between kinetic constants. Notably, circular dichroism experiments performed on WT and mutant PBP1b molecules did not identify any significant structural differences, even in the presence of antibiotic (data not shown).

In Streptococci, low β-lactam-affinity PBPs are present as highly mosaic molecules; PBP1a, -2x, and -2b are primary resistance determinants, and the presence of mutations throughout their entire TP domains is essential for the development of high-level resistance (10). Although PBP1b has not been linked to the development of resistance, the structure presented here can be used as a first framework for understanding how streptococci can develop resistance through mutation of PBP1a, with which PBP1b shares 45% sequence similarity within the TP domain. Mapping of mutations of a PBP1a from a highly penicillin-resistant streptococcal strain (9) onto the PBP1b* TP domain (Fig. 1) reveals three areas of particular interest. At the N terminus of α2, the SXXK motif (STTK) harbors the active site serine; mutation of the first threonine in the motif to alanine/serine may cause disruption of the hydrogen-bonding pattern within the cleft, as has been described for the identical mutation in PBP2x molecules from highly resistant

BIOCHEMISTRY

strains (24). In addition, the N terminus of α5, which immediately follows the SXN motif, displays a mutation of a highly conserved proline residue, which could affect stability of the α-helical chain. Lastly, a number of mutations are found within β4 and β5, which form the core of the conserved central β-sheet. High-resolution structures of PBP1a molecules from sensitive and resistant pneumococcal strains will be required to shed further light on this mechanism.

Analysis of the TP domain of PBP1b* reveals the most outstanding characteristic of the molecule: an activation phenomenon reflected in the existence of the active site gorge in closed and open conformations, the latter only possible in the presence of ligands. The two forms of PBP1b* were identified in two different space groups, which crystallized in the same solution and often in the same drop; no interactions generated by symmetry-related elements were observed in the active site regions. The opening and closing of the PBP1b* active site involve a substantial conformational modification, with substrate accessibility being blocked in the closed form. Ligand recognition requires that strands β3 and β4 be antiparallel in the active site area and that their interconnecting loop move away from the entrance of the cleft. This phenomenon was observed for both a large antibiotic molecule with a bulky, very hydrophilic R2 substitutent (nitrocefin) as well as for one with a minor R2 group (cefotaxime). Notably, in structures of β-lactamases and transpeptidases (including drug-resistant PBPs) reported to date, the antiparallel nature between β3 and β4 is always maintained in the presence or absence of ligands, and there is no dramatic blocking of the entrance of the cleft as seen here (compare the catalytic clefts in Fig. 5 *A* (closed) and *B* (open).

PBPs have been shown to play carefully orchestrated roles in cell division (4, 25–28). Recently, it has been reported that *E. coli* PBP3 (FtsI) becomes acylated at a faster rate in dividing cells than in nondividing cells, and the authors suggested that the enzyme's TP activity may become activated during septation (29). Based on those observations and our results reported here, we propose a model where PBPs could exist in nondividing cells in inactive ("closed") states. As their participation becomes essential within the cell-division cycle, PBPs would become active, either by recognizing substrate or by interacting with other members of a potential cell division or peptidoglycan elongation macromolecular complex. It is also possible that PBPs may exist in both closed and open conformations in the cell, the former switching into the latter depending on substrate availability or localization. Either way, the two forms of PBPs could provide the cell with a distinct handle on cell wall biosynthesis regulation.

We thank Marc Jamin for help with stopped-flow experiments, David Lascoux for mass spectrometry measurements, and the European Synchrotron Radiation Facility BM30 and ID14 staff for help with data collection. P.M. is a recipient of a CFR fellowship from the Comissariat à l'Energie Atomique. A.D. is an European Molecular Biology Organization Young Investigator. This work was supported by European Commission Grant LSHM-CT-2003-503335 (COBRA) and an ACI Jeunes Chercheurs grant from the French Ministry of Research (to A.D.).

1. Höltje, J. V. (1998) *Microbiol. Mol. Biol. Rev.* **62,** 181–203.
2. Goffin, C. & Ghuysen, J. M. (1998) *Microbiol. Mol. Biol. Rev.* **62,** 1079–1093.
3. Errington, J., Daniel, R. A. & Scheffers, D. J. (2003) *Microbiol. Mol. Biol. Rev.* **67,** 52–65.
4. Morlot, C., Noirclerc-Savoye, M., Zapun, A., Dideberg, O. & Vernet, T. (2003) *Mol. Microbiol.* **50,** 845–855.
5. Paik, J., Kern, Il, Lurz, R. & Hakenbeck, R. (1999) *J. Bacteriol.* **181,** 3852–3856.
6. Hoskins, J., Matsushima, P., Mullen, D. L., Tang, J., Zhao, G., Meier, T. I., Nicas, T. I. & Jaskunas, S. R. (1999) *J. Bacteriol.* **181,** 6552–6555.
7. Walsh, C. (2003) *Nat. Rev. Microbiol.* **1,** 65–70.
8. Smith, A. M. & Klugman, K. P. (2003) *Antimicrob. Agents Chemother.* **47,** 387–389.
9. Smith, A. M. & Klugman, K. P. (1998) *Antimicrob. Agents Chemother.* **42,** 1329–1333.
10. Hakenbeck, R., Konig, A., Kern, I., van der Linden, M., Keck, W., Billot-Klein, D., Legrand, R., Schoot, B. & Gutmann, L. (1998) *J. Bacteriol.* **180,** 1831–1840.
11. Di Guilmi, A. M., Dessen, A., Dideberg, O. & Vernet, T. (2003) *J. Bacteriol.* **185,** 1650–1658.
12. Otwinowski, Z. & Minor, W. (1997) *Methods Enzymol.* **276,** 307–326.
13. Terwilliger, T. C. & Berendzen, J. (1999) *Acta Crystallogr. D* **55,** 849–861.
14. Terwilliger, T. C. (1999) *Acta Crystallogr. D* **55,**1863–1871.
15. Navaza, J. (2001) *Acta Crystallogr. D* **57,** 1367–1372.
16. Brünger, A. T., Adams, P. D., Clore, G. M., DeLano, W. L., Gros, P., Grosse-Kunstleve, R. W., Jiang, J.-S., Kuszewski, J., Nilges, N., Pannu, N. S., *et al.* (1998) *Acta Crystallogr. D* **54,** 905–921.
17. Laskowski, R. A., MacArthur, M. W., Moss, D. S. & Thornton, J. M. (1993) *J. Appl. Crystallogr.* **26,** 283–291.
18. Lobkovsky, E., Moews, P. C., Liu, H., Zhao, H., Frere, J. M. & Knox, J. R. (1993) *Proc. Natl. Acad. Sci. USA* **90,** 11257–11261.
19. Kelly, J. A., Knox, J. R., Moews, P. C., Hite, G. J., Bartolone, J. B., Zhao, H., Joris, B., Frère, J. M. & Ghuysen, J. M. (1985) *J. Biol. Chem.* **260,** 6449–6458.
20. Parès, S., Mouz, N., Petillot, Y., Hakenbeck, R. & Dideberg, O. (1996) *Nat. Struct. Biol.* **3,** 284–289.
21. Sauvage, E., Kerff, F., Fonze, E., Herman, R., Schoot, B., Marquette, J.P., Taburet, Y., Prevost, D., Dumas, J., Leonard, G., *et al.* (2002) *Cell Mol. Life Sci.* **59,** 1223–1232.
22. Lim, D. & Strynadka, N. C. (2002) *Nat. Struct. Biol.* **9,** 870–876.
23. Di Guilmi, A. M., Mouz, N., Andrieu, J. P., Hoskins, J., Jaskunas, S. R., Gagnon, J., Dideberg, O. & Vernet, T. (1998) *J. Bacteriol.* **180,** 5652–5659.
24. Mouz, N., Gordon, E., Di Guilmi, A. M., Petit, I., Petillot, Y., Dupont, Y., Hakenbeck, R., Vernet, T. & Dideberg, O. (1998) *Proc. Natl. Acad. Sci. USA* **95,** 13403–13406.
25. Den Blaauwen, T., Aarsman, M. E. G., Vischer, N. O. E. & Nanninga, N. (2003) *Mol. Microbiol.* **47**, 539–547.
26. Daniel, R. A., Harry, E. J. & Errington, J. (2000) *Mol. Microbiol.* **35,** 299–311.
27. Pedersen, L. B., Angert, E. R. & Setlow, P. (1999) *J. Bacteriol.* **181,** 3201–3211.
28. Weiss, D. S., Chen, J. C., Ghigo, J. M., Boyd, D. & Beckwith, J. (1999) *J. Bacteriol.* **181,** 508–520.
29. Eberhardt, C., Kuerschner, L. & Weiss, D. S. (2003) *J. Bacteriol.* **185,** 3726–3734.
30. Kraulis, P. J. (1991) *J. Appl. Crystallogr.* **24,** 946–950.
31. Esnouf, R. M. (1999) *Acta Crystallogr. D* **55,** 938–940.
32. Nicholls, A., Sharp, K. A. & Honig, B. (1991) *Proteins* **11,** 281–296.
33. Gouet, P., Robert, X. & Courcelle, E. (2003) *Nucleic Acids Res.* **31,** 3320–3323.